

# QSAR modeling, docking and ADMET studies for exploration of potential anti-malarial compounds against *Plasmodium falciparum*

Tabish Qidwai<sup>1</sup>

Received: 8 April 2017 / Accepted: 8 July 2017  
© Springer-Verlag GmbH Germany 2017

**Abstract** Development of resistance in the *Plasmodium falciparum* to Artemisinin, the most effective anti-malarial compound, threatens malaria elimination tactics. To gain more efficacious Artemisinin derivatives, QSAR modeling and docking was performed. In the present study, 2D-QSAR model and molecular docking were used to evaluate the Artemisinin compounds and to reveal their binding modes and structural basis of inhibitory activity. Moreover, ADMET-related descriptors have been calculated to predict the pharmacokinetic properties of the effective compounds. The correlation expressed as coefficient of determination ( $r^2$ ) and prediction accuracy expressed in the form of cross-validated  $r^2$  ( $q^2$ ) of QSAR model are found 0.9687 and 0.9586, respectively. Total 239 descriptors have been included in the study as independent variables. The four chemical descriptors, namely radius of gyration, mominertia Z, SssNH count and SK Average have been found to be well correlated with anti-malarial activities. The model was statistically robust and has good predictive power which could be employed for virtual screening of proposed anti-malarial compounds. QSAR and docking results revealed that studied compounds exhibit good anti-malarial activities and binding affinities. The outcomes could be useful for the design and development of the potent inhibitors which after optimization can be potential therapeutics for malaria.

**Keywords** Anti-malarial activity · *Plasmodium falciparum* · QSAR · Docking · ADMET

## Introduction

Several millions of the people worldwide are infected by the *Plasmodium falciparum*, leading to death of around 1 million annually (World Malaria Report 2013). Most of the therapeutic approaches are Artemisinin based combination therapies (ACTs) and chloroquine (Fidock et al. 2004). Semi-synthetic derivatives of Artemisinin are more frequently used in malaria chemotherapy, due to their better pharmacokinetic properties and higher efficacies as compared to parent compound. ACT is fast acting, well tolerated and is nearly 95% effective in the treatment of malaria. However resistance in parasite to ACTs has been reported in some south-east Asian countries (Kar and Kar 2010). As the *P. falciparum* resistance to Artemisinin has emerged, development of novel effective anti-malarial drugs is an urgent priority. It prompted to explore further efficient drug like compounds with new mechanisms of action. Currently, quantitative structure activity relationship (QSAR) is useful to check time consumption and cost throughout the analysis of biological activities (Ibezim et al. 2012). Since last few years, QSAR modeling became an important tool for drug design and structural optimization (Bhatarai and Garg 2008; Xiang et al. 2009; Basak et al. 2010) and is widely used for virtual screening of compounds.

In the current study, molecules with wide range of activities (activity range of 1.4–10,630 nano molar) were used to understand the distinct contributing features for their high potency. The present work describes the development of a QSAR model by using multiple linear

**Electronic supplementary material** The online version of this article (doi:10.1007/s40203-017-0026-0) contains supplementary material, which is available to authorized users.

✉ Tabish Qidwai  
tabish.qidwai@gmail.com

<sup>1</sup> Department of Biotechnology, Babasaheb Bhimrao Ambedkar University, Lucknow 226025, India

regression analysis (MLRA) technique which successfully and accurately predicted activity modulating descriptors. The developed model was used to screen Artemisinin derivatives and to predict the activity. The 11 compounds were identified with very good anti-malarial activities (less than 0.5 nano molar log IC<sub>50</sub>). Also, the pharmacokinetic properties were predicted through calculation of the absorption, distribution, metabolism, excretion and toxicity (ADMET) related descriptors. Furthermore, through docking possible binding sites and conserved pockets were identified for active compounds against plasmepsin-2 and falcipain-2 of the *P. falciparum*. It will be useful for understanding the molecular mechanism and directing the molecular design of more potent Artemisinin based inhibitors.

## Materials and methods

### QSAR model development

The QSAR study was performed using a series of Artemisinin derived compounds reported in the literature (Qidwai et al. 2012; Yadav et al. 2014; Posner et al. 1999; O'Neill et al. 2001; Avery et al. 2003; Liu et al. 2011). The biological activities were represented by the log IC<sub>50</sub>. The data set of 47 Artemisinin derivatives which were randomly divided in training set (32 compounds) for model development and test set (15 compounds) for model validation. The seventy percent training and thirty percent test set compounds were maintained during the analysis. The chemical structures and their biological activities have been shown (Supp Table 1). The V-life MDS (Molecular Design Suite) TM 3.5 software, supplied by V-life Sciences Technologies was used to build QSAR model (V-life MDS software package, version 3.5 2008).

### Ligand preparation and optimization

The molecular structures of all of the molecules were sketched using the ChemBioDraw-Ultra-v12.0 (2010) software. The chemical structures of known drugs were retrieved from the PubChem compound database, which is available at NCBI (<http://www.pubchem.ncbi.nlm.nih.gov>). Three dimensional geometry of the compounds was generated using Accelrys Discovery Studio (DS) v3.1 (Software Inc., San Diego, CA, USA).

### Descriptor calculation

A large number (239) of theoretical two dimensional descriptors were selected for QSAR analysis. The descriptors that have been computed from chemical

structures to identify structure/activity relationship of Artemisinin compounds are vdW surface area (van der Waals surface area of the molecule), ve potential surface area (total van der Waals surface area with negative electrostatic potential of the molecule), +ve potential surface area (total van der Waals surface area with positive electrostatic potential of the molecule) dipole moment, Y compDipole (y component of the dipole moment), element count, slogP, path count, cluster, distance based topological indices, connectivity index, hydrophobic and hydrophilic areas like SA most hydrophilic (most hydrophilic value on the vdW surface by Audry method using Slogp), SA most hydrophobic–hydrophilic distance (distance between most hydrophobic and hydrophilic point on the vdW surface by Audry method using Slogp), SA hydrophilic area (vdW surface descriptor showing hydrophilic surface area by Audry method using SlogP) and SK most hydrophilic (most hydrophilic value on the vdW surface by Kellog method using Slogp), radius of gyration, Wiener's index, moment of inertia, semi-empirical descriptors, HOMO (Highest occupied molecular orbital), LUMO (lowest unoccupied molecular orbital), heat of formation and ionization potential, polarizability AHC, Chi1, Chi2, polar surface area, radius of gyration, Mom InertiaZ, SssNH count, SK average, MomInertia X, MomInertia Y, MomInertia Z.

### Cross validation

The models generated by two dimensional QSAR studies were cross validated using a standard leave one out (LOO) procedure. The cross validated coefficient of determination ( $r^2$ ) i.e.  $q^2$  value was calculated. The  $q^2$  obtained is indicative of the predictive power of the current model. The  $q^2$  was calculated using Eq. (1).

$$q^2 = 1 - \frac{\sum (y_i - \hat{y}_i)}{\sum (y_i - y_{\text{mean}})^2} \quad (1)$$

$$\text{Pred}_r^2 = 1 - \frac{\sum (y_i - \hat{y}_i)}{\sum (y_i - y_{\text{mean}})^2} \quad (2)$$

The external predictive power of the model is assessed by predicting the log IC<sub>50</sub> value of test set molecules, which were not included in the QSAR model development. The predictive ability of the selected model was confirmed by pred  $r^2$ . The selected descriptors were then used to build QSAR model.

### Molecular docking studies

Molecular docking was carried out with the help of Glide module of Schrodinger (2016) and PyRx (Autodoc vina) (Trott and Olson 2010). Three dimensional structures of

target proteins were retrieved from Protein Data Bank (PDB) (<http://www.pdb.org>). The Artemisinin derivatives were docked to the crystal structures of plasmepsin-2 (PDB code: 2IGY) and falcipain-2 (PDB code: 3BPF).

### Protein preparation

The protein preparation wizard from Schrodinger was used to prepare protein structure retrieved from the PDB. Hydrogen atoms were added to the protein structures corresponding to pH value of 7.4. All-atom constrained energy minimizations were carried out using the OPLS-2005 force field. An energy minimization was terminated when the root mean square deviation (RMSD) was larger than 0.30 Å.

### Ligand preparation for docking

All ligands for docking were prepared using LigPrep module of Schrodinger (2016) by generating low energy ionization and tautomeric states within the pH range of  $7.4 \pm 0$ . They were further minimized using the OPLS-2005 force field.

### Receptor grid generation and docking

Docking is based on a grid represented by physical properties in the receptor volume that is searched for ligand-receptor interaction during docking process. Glide uses a grid file to describe the profile of a binding pocket, with the center of the grids defined by the co-crystallized ligand. Grid files were prepared with the "Receptor Grid Generation" panel of Glide. Grid points were calculated within a region or an enclosing box defined with the centroid of the bound ligand and the size of a docked ligand with length  $\leq 20$  Å. Docking was performed by Glide of Schrodinger (2016). The score function of Glide, or Glide score, was used for binding affinity prediction.

### ADMET studies

ADMET profiling of compounds were performed by applying ADMET descriptors algorithm and toxicity prediction protocol of Qikprop of Schrodinger (2016) and ADMETSAR database (freely available at <http://www.admetexp.org>) (Cheng et al. 2012).

### Results

The best QSAR model was selected on the basis of predicted fitness plots and statistical values of the model. The developed model is found with coefficient of determination ( $r^2$ ), cross-validated  $r^2$  ( $q^2$ ) and the  $r^2$  for external test set

( $\text{pred}_r^2$ ) values of 0.9687, 0.9586 and 0.9247 respectively. Standard error of estimate (SEE)  $r^2$  ( $r^2_{se}$ ) and standard error of estimate (SEE)  $q^2$  ( $q^2_{se}$ ) are predicted 0.2206 and 0.2535 respectively. The statistical significance of the model (F-test) is 208.58 and degree of freedom (df) is found 32. The linear and radar plots of experimental versus predictive  $\log IC_{50}$  values of compounds in training and test data set are depicted in Figs. 1, 2 respectively. The descriptors based on the model used in the present study are indicated (Fig. 3). Figure 4 depicts two dimensional structures of proposed Artemisinin compounds. QSAR model based predicted properties of Artemisinin compounds are illustrated in Table 1.

In this study, flexible docking was performed using the extra precision (XP) mode in Glide with the default settings. The improvement of XP over standard precision (SP) mode includes the addition of large desolvation penalties to both ligand and protein, assignment of specific structural motifs that give significantly to binding affinity, and expanded sampling algorithms required by scoring function improvement. The XP scoring function includes four constituents:  $E_{\text{coul}}$  (Coulomb energy),  $E_{\text{vdw}}$  (Van de Waals' energy),  $E_{\text{bind}}$  (items favouring binding), and  $E_{\text{penalty}}$  (items hindering binding). To cross check whether docking protocol is working fine, deviation from crystal pose and

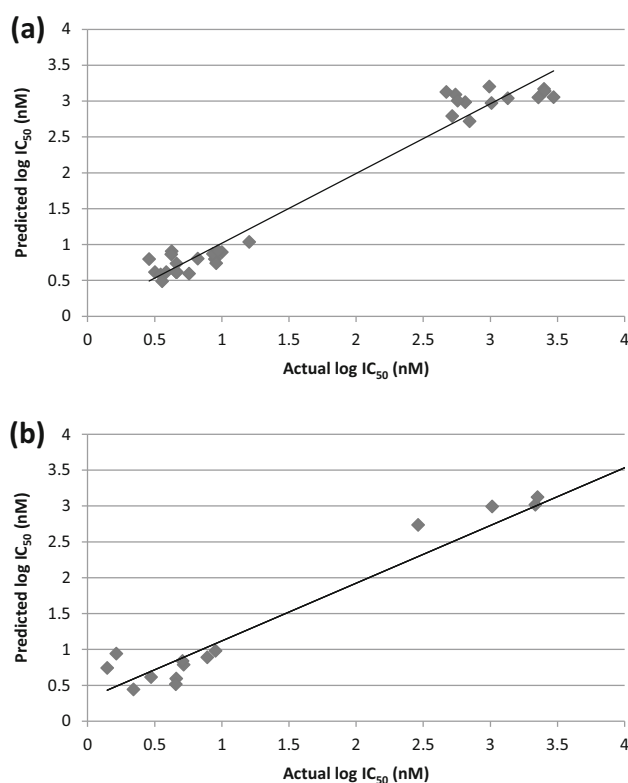


**Fig. 1** Multiple linear regression plot expressing the experimental and predicted  $\log IC_{50}$  values for the training (a) and test (b) set compounds

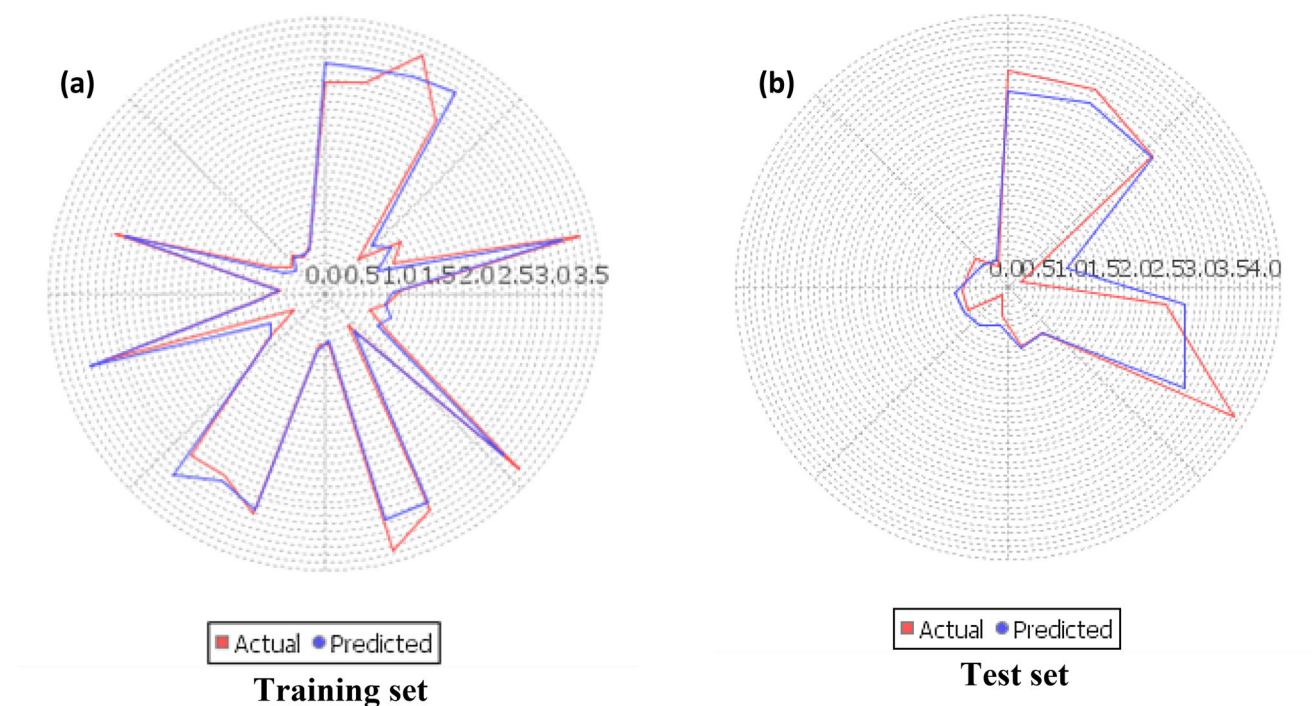


**Fig. 2** The radar plots denoting the training (a) and the test (b) sets by the red (actual activity) and blue (predicted activity) lines

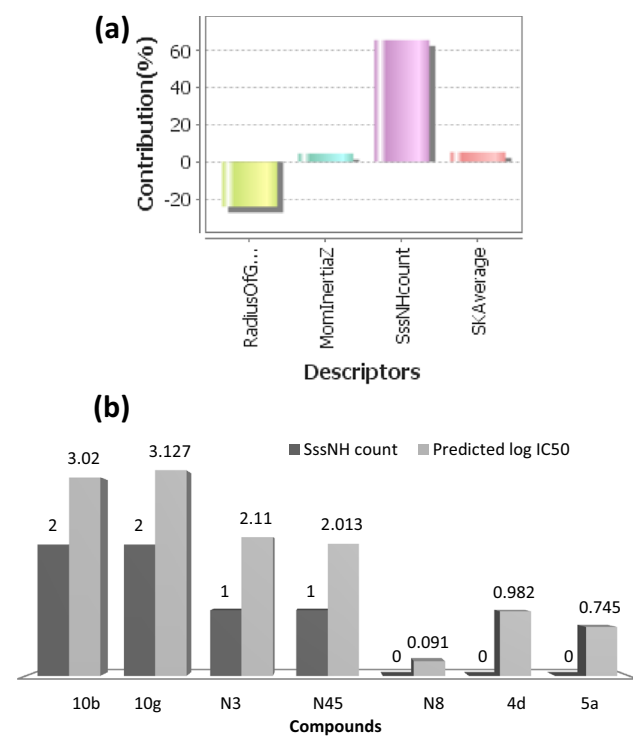


**Fig. 3** a Four descriptors, radius of gyration (geometrical descriptor), Mom inertia Z (topological descriptor), SssNH count (sum of ssNH-electrotopological-states), a topological descriptor and SK average (semi-empirical descriptors) have been shown correlation with anti-malarial activity. b Anti-malarial activity (log IC<sub>50</sub>) modulation by topological descriptor SssNH count

docked pose was measured by RMSD. The measured deviation should not be more than 2 Å. Tables 2 and 3 illustrate the docking scores resulting from the docked poses of ligands with the anti-malarial targets, plasmepsin-2 and falcipain-2. Figure 5 shows the two and three dimensional ligand-interaction diagram illustrating the major interactions between the ligand and the active sites amino acid residues of plasmepsin-2.

The predicted pharmacokinetic properties of the studied compounds are presented in the Tables 4 and 5.

## Discussion

In an attempt to determine the role of structural features, which appears to influence the anti-malarial activity, QSAR study is important. The predicted QSAR model showed good predictivity as it satisfies the required parameters. For evaluation of the external predictive power of the model, it was applied for the prediction of log IC<sub>50</sub> values of test set which was not part of training set during model development. The linear graphical representation of fitness plots illustrates the good overlap of observed and predicted activities of the data set (Fig. 1). The radar plot for training set shows a good  $r^2$  value as the two lines show a good overlap whereas a good overlap for the test set represents high  $\text{pred}_r^2$  value (Fig. 2). The statistical output of this model is presented as following:

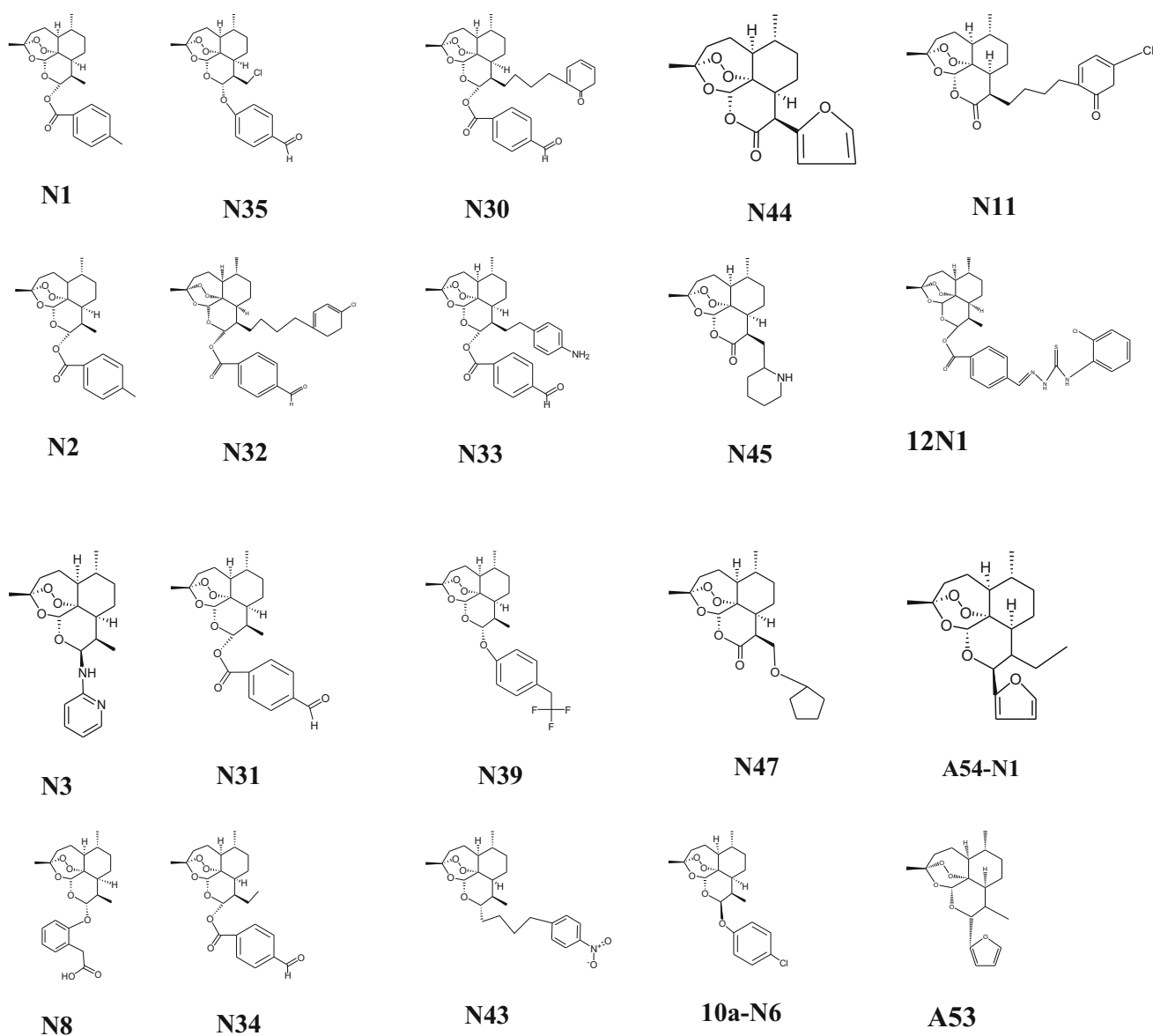


**Fig. 4** The above figure depicts two dimensional structures of proposed Artemisinin compounds

$$\begin{aligned}
 \text{Output} = & (-0.0338 \times \text{Radius of Gyration}) \\
 & + (0.0000 \times \text{Mom Inertia Z}) \\
 & + (1.7504 \times \text{SssNH count}) \\
 & + (0.9462 \times \text{SK Average}) + 0.0028.
 \end{aligned}$$

The robustness and the predictive capacity of the QSAR model were predicted through the statistical parameters. QSAR studies are affected by several factors from which the most important are: (i) the selection of the best molecular descriptors that should include maximum information of molecular structures and a minimum overlap between them (ii) the optimal number of descriptors to be included in the model (Ibezim et al. 2012). The

descriptors are commonly used to express different characteristics/attributes of the chemical structure in order to give information about the activity/property being studied. The developed model has identified four descriptors, radius of gyration (geometrical descriptor), Mom inertia Z (topological descriptor), SssNH count (sum of ssNH-Electrotopological-states), a topological descriptor and SK average (semi-empirical descriptors) that have been found to be well correlated with anti-malarial activity. The descriptor SssNH count is produced marked change in anti-malarial activity of the studied compounds. The log IC<sub>50</sub> of the compounds radically increases with descriptor SssNH count (Fig. 3b). The compounds 4c, d, 5a–24, 5a, b, 6, 9b, DHA and Artemether are highly active compounds have

**Table 1** Compounds (Artemisinin derivatives) selected for the QSAR study and their predicted properties

Molecules	Exp. log IC <sub>50</sub> (nm)	Predicted log IC <sub>50</sub> (nm)	Radius of gyration	Mom inertia Z	SssNH count	SK average
10b <sup>a</sup>	3.336	3.02	45.474	260,684.135	2	0.73
10g <sup>a</sup>	3.352	3.127	41.864	258,525.502	2	0.718
10k <sup>a</sup>	3.013	2.996	46.571	255,952.04	2	0.752
11 <sup>a</sup>	0.215	0.944	8.812	253,845.862	0	0.936
12c <sup>a</sup>	2.462	2.737	52.683	264,789.63	2	0.683
12f <sup>a</sup>	4.027	3.145	44.711	300,574.845	2	0.777
4c <sup>a</sup>	0.892	0.894	8.332	188,117.998	0	0.962
4d <sup>a</sup>	0.954	0.982	9.121	238,612.036	0	1.009
5a-24 <sup>a</sup>	0.473	0.617	7.958	53,611.206	0	0.855
5a <sup>a</sup>	0.146	0.745	6.034	158,687.583	0	0.766
5b <sup>a</sup>	0.716	0.79	6.467	167,619.915	0	0.816
6 <sup>a</sup>	0.708	0.842	6.102	167,478.081	0	0.858
9b <sup>a</sup>	0.661	0.595	8.141	54,629.07	0	0.836
Artemether <sup>a</sup>	0.658	0.517	4.874	98,526.224	0	0.572
DHA <sup>a</sup>	0.342	0.444	3.858	92,237.768	0	0.469
A53		0.594	11.286	242,119.5	0	0.672
A54-N1		0.722	10.52	244,511.2	0	0.776
A54		0.654	10.27	232,279.5	0	0.713
A62		0.44	9.374	205,296.2	0	0.494
N1		0.334	17.551	200,410.966	0	0.682
N2		0.334	17.551	200,410.966	0	0.682
N3		2.11	13.808	178,682.195	1	0.607
N5		0.835	18.853	295,673.337	0	1.118
N8		0.091	24.026	222,484.454	0	0.624
N11		0.705	12.689	186,863.092	0	0.92
N17		0.83	10.374	172,287.408	0	0.991
N22		0.518	10.048	145,306.119	0	0.69
N23		0.716	4.29	103,242.677	0	0.755
N30		0.397	24.47	281,172.89	0	0.877
N31		0.189	19.247	184,155.601	0	0.614
N32		0.515	26.855	299,622.463	0	1.06
N33		0.404	20.668	254,465.477	0	0.787
N34		0.311	18.854	216,043.634	0	0.682
N35		0.347	17.926	211,990.211	0	0.692
N36		0.551	21.425	272,614.106	0	0.943
N37		0.696	27.47	337,035.527	0	1.218
N38		0.54	18.066	228,358.346	0	0.877
N39		0.193	26.45	225,217.086	0	0.815
N43		0.408	23.059	236,491.738	0	0.904
N44		0.394	10.449	159,053.153	0	0.552
N45		2.013	13.004	178,032.21	1	0.477
N47		0.222	15.898	186,829.202	0	0.525
10a-N6		0.355	19.734	204,537.942	0	0.777
12-N1		3.25	41.257	296,730.481	2	0.77

<sup>a</sup> Test compounds



**Table 2** Docking and energy calculation results of potent Artemisinin derivatives against plasmepsin-2

Compounds	Glide score	Glide energy
A2T (crystal ligand)	-10.895	-93.678
N30	-9.224	-80.836
N32	-9.051	-64.257
N39	-8.342	-45.534
12f	-7.889	-57.929
N8	-7.458	-56.81
N47	-7.04	-46.242
N1	-6.159	-42.097
A53	-6.09	-33.931
N2	-6.008	-42.762
N31	-5.732	-52.009
A54	-5.097	-28.057
N45	-4.714	-30.696
N3	-4.432	-35.244
DHA	-4.011	-30.894
Deoxy-Artemisinin	-3.904	-21.788
Artemisinin	-2.795	-32.612
A62	-2.326	-5.349

SssNH count zero and lower radius of gyration values as compared to the compounds 10b, g, k, 12c, 12f. The N8 which is the most active compound has been predicted with zero SssNH count whereas compounds 12f and 12N1 (the

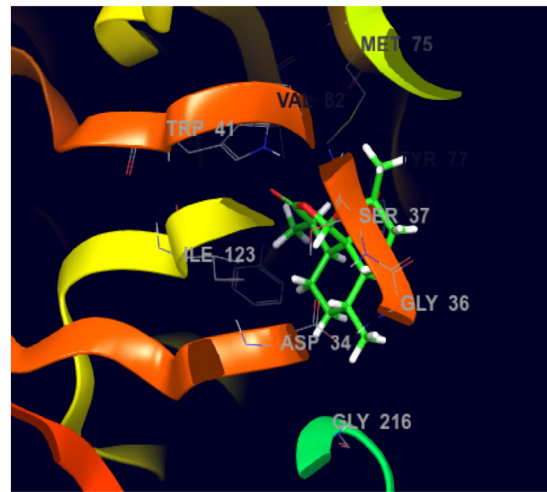
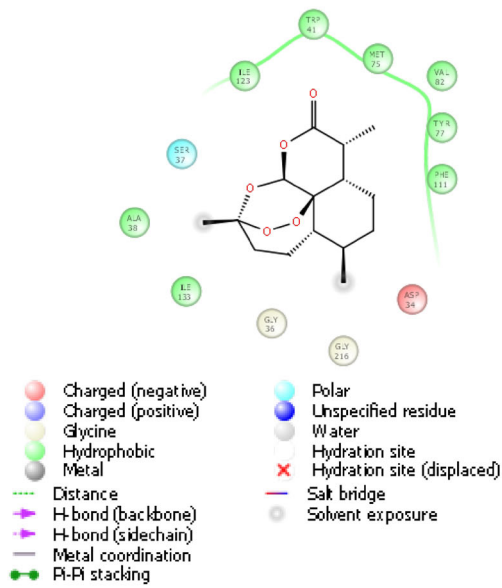
least active) are predicted to have two SssNH count. In this context, it was of interest to estimate the effect of this descriptor on the anti-malarial potential of structurally diverse Artemisinin compounds. The results of virtual screening show that 11 compounds (N1, N2, N8, N30, N31, N33, N34, N35, N39, N47 and 10a-N6) are found to have potential anti-malarial activities. Further, compound N8 has great potential of being lead as it has highest predicted activity and also has good binding affinity to both targets (Table 3). Although previous studies were carried out to explore the activity modulating effect of various descriptors in the Artemisinin however in the present study, the predicted descriptors are new that allow a better understanding of the structure of molecules and their activity. Also, the designed and virtually screened compounds are new. The selected Artemisinin compounds have good anti-malarial activities and have greater potential of being drug after optimization.

### Molecular docking studies

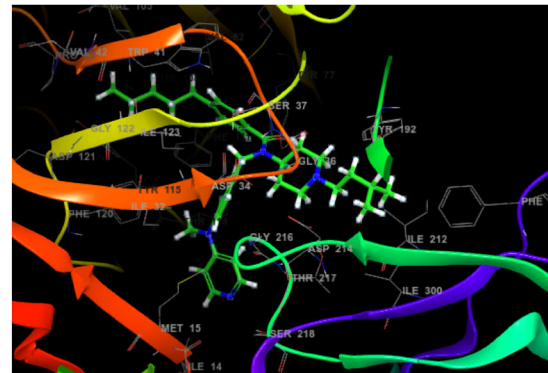
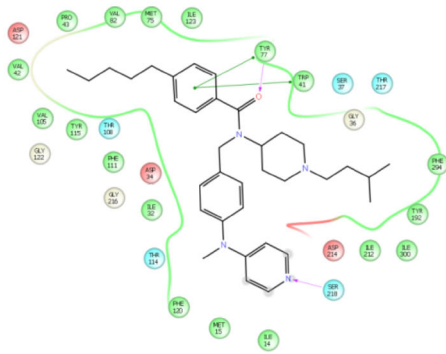
Although several studies have been done to unravel mode of action of Artemisinin, still exact mechanism is confusing (Golenser et al. 2006) and it is under investigation. Eckstein-Ludwig et al. (2003) assumed that Artemisinin act by inhibiting *P. falciparum* ATP6 outside the food vacuole after activation by iron. Artemisinin has structural similarities to thapsigargin, an immensely precise inhibitor of

**Table 3** Comparison of binding affinities of active Artemisinin based compounds with anti-malarial targets, plasmepsin-2 (2IGY) and falcipain-2 (3BPF)

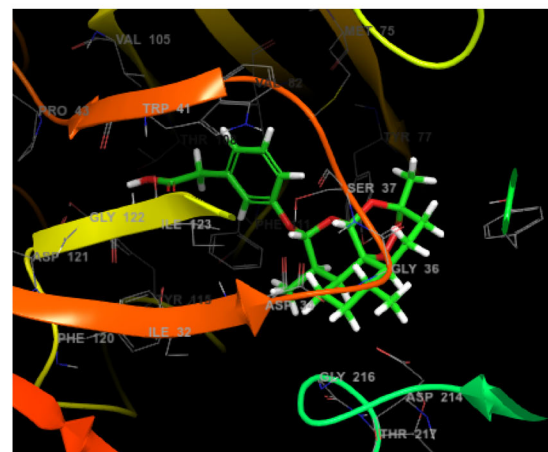
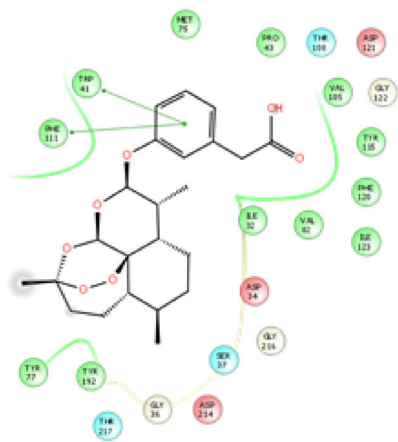
Protein-ligand	Binding energy (kcal/mol)	Protein-ligand	Binding energy (kcal/mol)
2IGY_A53	-6.8	3BPF_A53	-7.9
2IGY_A54	-6.9	3BPF_A54	-7.8
2IGY_A62	-6.7	3BPF_A62	-7.2
2IGY_A54-N1	-6.8	3BPF_A54-N1	-7.7
2IGY_Artemether	-6.5	3BPF_Artemether	-6.6
2IGY_Artemisinin	-6.6	3BPF_Artemisinin	-6.8
2IGY_DHA	-6.6	3BPF_DHA	-6.6
2IGY_N11	-7.7	3BPF_N11	-9.6
2IGY_N2	-7.7	3BPF_N2	-8.6
2IGY_N8	-8.2	3BPF_N8	-9.1
2IGY_N30	-9.2	3BPF_N30	-10.8
2IGY_N33	-8.2	3BPF_N33	-8.5
2IGY_N39	-8.6	3BPF_N39	-9.5
2IGY_N43	-8.1	3BPF_N43	-9.6
2IGY_N44	-7.3	3BPF_N44	-8.2
2IGY_N45	-7.9	3BPF_N45	-8.7
2IGY_N47	-7.6	3BPF_N47	-8.1
2IGY_Deoxyartemisinin	-6.6	3BPF_Deoxyartemisinin	-7
2IGY_12F	-10.3	3BPF_12F	-11.4



### Artemisinin



### A2T (2IGY)



### N8

**Fig. 5** The ligand-interaction diagram illustrates the major interactions between the ligand and the active sites amino acid residues of plasmepsin-2 (PDB: 2IGY). The residues forming the potential interactions are shown as colour





sarco/endoplasmic reticulum  $\text{Ca}^{2+}$ -ATPase (SERCA). Studies suggested that Artemisinin likely targets to the *P. falciparum* cysteine protease and aspartic protease (Qidwai et al. 2012; Eckstein-Ludwig et al. 2003; Ettari et al. 2010). In human erythrocytes, the malaria parasite hydrolyses host hemoglobin for its amino acid requirement. The hemoglobin degradation is carried out by three classes of enzymes named as plasmepsin, falcipain and amino-peptidases and their inhibition may block parasite protein biosynthesis and leading to harmful effect to the parasite (Rosenthal et al. 2002). Therefore, targeting of these enzymes would be important for malaria treatment and can be utilized as potential anti-malarial drug targets. In order to understand the interaction of Artemisinin derivatives with parasite hemoglobinase (plasmepsin-2 and falcipain-2), docking was performed (Table 2). Docking protocol was checked by RMSD calculations. Deviation from crystal and docked pose was measured.  $\text{RMS} = 1.0111$ ; maximum  $\text{diff} = 3.2469$  between atoms 65 and 65 have been predicted. The result of study suggested that studied compounds have good binding affinities to plasmepsin-2 and falcipain-2 (Tables 2, 3). The docked compound N30 has been found with highest binding affinity as predicted by both Glide and PyRx. Similarly, the docked ligand N39 has good binding affinity. Both ligands also have good predicted anti-malarial activities. Comparison of binding affinities of Artemisinin compounds with two anti-malarial targets suggested that the binding affinities are higher for falcipain-2 as compared to plasmepsin-2. The results showed that, studied compounds having minimum binding energy and have good affinity toward the active pocket, thus, they may be considered as good inhibitor of *P. falciparum* proteases digesting host hemoglobin. Results showed that all the derivatives showed interaction in the active binding pocket of targets and have higher binding affinity as compared to the standard drugs DHA and Artemisinin. QSAR and docking work suggested that the compounds N30 and N39 have great potential of being drug like compounds after optimization against *P. falciparum*.

#### Artemisinin may not target to parasite hemoglobinase

The idea that Artemisinin may not acts via targeting to parasite proteases came through the docking of Deoxy-artemisinin. Deoxy-Artemisinin has no effect on *P. falciparum* and does not inhibit its growth. However, docking energies resulting from the interaction of Deoxy-artemisinin-plasmepsin-2 and Deoxy-artemisinin-falcipain-2 have been predicted nearly equal to that of interaction of Artemisinin-plasmepsin-2 and Artemisinin-falcipain-2. The  $\text{IC}_{50}$  values of compound 12f (the least active compound in the model) and Artemisinin are 10,630 and 3.6 nM

respectively. The binding affinities of plasmepsin-2 and falcipain-2 with compound 12f are higher than their binding affinities with Artemisinin (Table 3). It seems that Artemisinin and its derivatives may exert their effect through either binding with another target or with multiple targets. Deoxy-artemisinin and 12f docking results may not support that Artemisinin specifically binds to protein and inhibits it. Artemisinin and other members of this class that encompass the peroxide bond, may interact with the electron transport chain of malaria parasites, make free radicals, which could damage mitochondrial functions and ultimately lead to cell death (Wang et al. 2010). Probably Artemisinin does not perform its functions through binding precisely to protein target site and then inhibiting its function. The anti-malarial effect of Artemisinin is due to its selective interaction with malarial mitochondria, which makes reactive oxygen species. The peroxide bond of the molecule is vital to the production of free radicals.

#### Absorption, distribution, metabolism, excretion, and toxicity studies

During the drug discovery effort many drugs are miscarried due to blood brain permeation failure, toxicity and poor efficacy. Since Artemisinin possess anti-malarial activity and it has poor pharmacokinetic properties, therefore virtual derivatives were designed and properties were investigated. Absorption, distribution, metabolism, excretion, and toxicity (ADMET) properties are key players in drug development. Lack of efficacy and unacceptable toxicity are mainly associated with failures of drug discovery. Suitable lipophilic property is important for the drugs to cross membrane and cytosol to reach the target. The ADMET-related properties for instance water solubility, human intestinal absorption, oral bioavailability, blood brain barrier (BBB) penetration, transporter, plasma protein binding, volume of distribution, CYP450, toxicity are used to refine the drug likeness properties (Vlife and software package, version 3.5 2008). In the present study, ADMET properties of the Artemisinin and its derivatives were predicted through ADMETSAR database which is freely available. Several ADMET associated properties, such as water solubility, human intestinal absorption, oral bioavailability, blood brain barrier penetration, P-glycoprotein substrate and inhibitor, renal organic cation transporter, plasma protein binding, volume of distribution, CYP450 substrates and inhibition (CYP1A2, 2C9, 2C19, 2D6 and 3A4), drug-induced liver injury, human Ether-a-go-go-Related gene (hERG) inhibition, rat acute toxicity, skin sensitivity, AMES mutagenicity, carcinogens, fish toxicity, the *Tetrahymena pyriformis* toxicity have been predicted. For Artemisinin probabilities of being human intestinal absorption, blood-brain barrier penetration,

**Table 4** Compliance of active Artemisinin compounds to electronic parameters of drug likeness and toxicity

Compounds	ADME descriptors and their probabilities											
	BBB+	HIA+	Caco2+	CYP	CYP1P	HERGI	Non AMES toxicity	Non carcinogens	Fish toxicity	Aqueous solubility (LogS)	Caco-2 permeability	Rat acute toxicity
Artemisinin	0.9490	0.9747	0.8867	0.8493	0.9850	0.9711	0.7785	0.9161	0.8911	-4.3515	1.3569	1.7351
Artemether	0.9393	0.9012	0.7876	0.8665	0.9672	0.9502	0.7285	0.9179	0.6930	-4.7024	1.1659	2.2114
DHA	0.9530	0.7795	0.7545	0.8046	0.9857	0.9608	0.8011	0.7825	0.9220	-4.5379	1.1277	2.2266
A62	0.9645	0.9824	0.7804	0.8637	0.9563	0.9597	0.7310	0.9006	0.9384	-4.5002	1.2038	2.0254
N2	0.9521	0.9857	0.6306	0.8667	0.7729	0.9444	0.8125	0.8782	0.9865	-5.0688	1.0673	2.3350
N8	0.9364	0.8929	0.5784	0.8100	0.9686	0.9405	0.7448	0.9037	0.9915	-5.1502	0.8055	2.5428
N11	0.9389	0.9573	0.5912	0.8828	0.8746	0.8673	0.7606	0.9184	0.9927	-4.6707	0.8752	2.4281
N30	0.9382	0.9506	0.5979	0.8567	0.7699	0.8846	0.8020	0.9377	0.9942	-4.9804	0.6902	2.5728
N33	0.9251	0.8499	0.5439	0.8746	0.8030	0.9598	0.6797	0.9041	0.9851	-4.4100	0.5692	2.5515
N35	0.9653	0.9928	0.6238	0.8176	0.8500	0.9259	0.8015	0.8670	0.9921	-4.8652	0.9049	2.5546
N39	0.9839	0.9917	0.5936	0.8628	0.8498	0.8524	0.7201	0.8579	0.9951	-5.4983	0.8585	2.6161
N40	0.9768	0.9952	0.6577	0.8670	0.9123	0.9061	0.7384	0.8585	0.9923	-5.4400	1.0206	2.4757
N41	0.9401	0.9710	0.7546	0.8668	0.9118	0.9073	0.7379	0.9328	0.9567	-4.8319	1.1453	2.2262
N42	0.9856	0.9909	0.6371	0.8617	0.8666	0.8730	0.6689	0.7916	0.9681	-4.8343	1.0292	2.5175
N44	0.9354	1.0000	0.7251	0.8311	0.9069	0.9769	0.8510	0.9250	0.9966	-4.4386	1.0854	2.7435
N45	0.9785	0.9886	0.5413	0.8911	0.9611	0.9635	0.7025	0.9429	0.7752	-3.3146	0.8619	2.6761
N46	0.9507	0.8525	0.5825	0.7821	0.9491	0.9098	0.6025	0.6678	0.7923	-3.8902	0.6514	2.4344
N47	0.9773	0.9682	0.5798	0.8706	0.8898	0.9726	0.8441	0.9345	0.9316	-4.2629	0.8923	2.4667
10a-N5	0.5501	0.6140	0.5746	0.6832	0.6036	0.8597	0.5448	0.7064	0.9972	-4.2729	0.4760	2.6962
12N1	0.5446	0.6527	0.5727	0.7150	0.5359	0.9336	0.5703	0.7135	0.9997	-4.3700	0.5885	2.7064

BBB+ blood brain barrier, HIA+ human intestinal absorption, Caco2+ Caco-2 permeability, CYP CYP450 2C9 substrate, CYP1P CYP inhibitory promiscuity, HERGI human ether-a-go-go-related gene inhibition, LogPapp, cm/s Caco-2 permeability, LD50, mol/kg rat acute toxicity

**Table 5** Calculation of electronic parameters of drug likeness or oral bioavailability of the Artemisinin compounds by using Qikprop

Molecule	Mol. MW	HB donor	HB acceptor	QPPCaco	QPlogBB	QPPMDCK	Percent human oral absorption	PSA	N & O	Rule of five	Ring atoms
Artemisinin	282.336	0	5.25	2010.388	0.009	1052.349	96.213	64.326	5	0	16
DHA	284.352	1	5.65	2155.001	-0.057	1134.403	100	57.405	5	0	16
Deoxy arte	266.336	0	4.5	3397.191	0.197	1855.359	100	52.716	4	0	15
N1	402.486	0	5.95	2676.943	-0.124	1434.093	100	64.666	6	0	22
N2	402.486	0	5.95	2676.95	-0.124	1434.097	100	64.666	6	0	22
N8	418.486	1	6.7	153.32	-0.944	82.893	90.445	92.136	7	0	22
N31	416.47	0	7.95	494.467	-0.918	231.073	90.917	101.904	7	0	22
N34	430.497	0	7.95	510.069	-0.987	238.964	93.358	101.731	7	0	22
N35	422.905	0	6.7	1092.874	-0.442	1106.213	100	76.926	6	0	22
N38	470.485	0	6.7	1034.505	-0.479	2176.841	100	78.647	6	0	22
N39	442.474	0	4.7	5916.921	0.425	10,000	100	40.733	5	1	22
N45	365.469	1	6.75	397.627	0.091	201.981	87.477	76.157	6	0	22
N47	366.453	0	6.95	2021.644	-0.254	1058.719	100	71.315	6	0	21
10a-N5	556.057	2	6.7	536.357	-0.93	1085.364	84.149	99.09	9	2	28
12-N1	600.128	2	9.95	1084.579	-0.713	2525.4	89.829	106.742	9	2	28
12f	598.094	2	7.95	325.389	-1.3	531.102	80.017	127.055	10	2	28

HB hydrogen bond, QPlogBB brain/blood partition coefficient, QPPMDCK apparent MDCK cell permeability, PSA polar surface area

CYP450 substrates and inhibition, human Ether-a-go-go-Related gene (hERG) inhibition and AMES mutagenicity, carcinogenicity, fish toxicity, aqueous solubility (LogS), Caco-2 Permeability and rat acute toxicity have been found 0.9747, 0.9490, 0.8493, 0.9850, 0.9711, 0.7785, 0.9161, 0.8911, -4.3515, 1.3569 and 1.7351 respectively. The detailed predicted properties of other studied compounds with respect to Artemisinin artemether and DHA have been shown (Table 4). Blood–brain barrier penetration probabilities of compounds N2, N22, N35, N39, N40, N42, N45, N46 and N47 are higher than Artemisinin and artemether while such probabilities have been found lower for compounds 10a-N5 and 12N1. Probabilities of human intestinal absorption for N35, N39, N40, N42 and N45 are higher than Artemisinin, DHA and artemether while lower for compounds 10a-N5 and 12N1. Compounds N30, N35, N44 and N47 have been predicted with higher probabilities of Non AMES Toxicity as compared to A62, Artemisinin and artemether. Compounds N2, N8, N33, N35, N39, N40 and N42 have been found to be carcinogens with lower probabilities. Compound N8 has 90% probability of not possessing mutagenic properties and 74% chance of being non AMES toxic. Proposed compounds have been found with better ADME properties, therefore have greater potential of being lead compounds.

Further, pharmaceutically significant properties of Artemisinin analogs were analyzed through QikProp software (Table 5) and compared them with standard drugs, Artemisinin, artemether and DHA. The results predicted through QikProp suggested that compounds N2, N8, N33, N35, N39, N40 and N42 have been found with good ADME properties. The major descriptors reported in QikProp (Schrodinger) software are molecular weight (mol\_MW) (150–650), aqueous solubility (QPlogS) (–6.5 to 0.5), apparent MDCK cell permeability (QPPMDCK) (500 great), brain/blood partition coefficient (QPlogBB) (–3.0 to 1.2) and percent human oral absorption ( $\geq 80\%$  is high,  $\leq 25\%$  is poor). All the studied compounds have percent human oral absorption 80–100% (Table 5). The first three properties are based on Lipinski rule of five, molecular weight (mol\_MW) less than 650, partition coefficient between octanol and water (logPo/w) between –2 and 6.5 and solubility (QPlogS) greater than –7. Brain/blood partition coefficient (QPlogBB) parameter specified about the capacity of the drug to pass through the blood–brain barrier which is important for ADME for investigating druggability. Lipinski's rule of five pharmacokinetics filter is used as a drug likeness test. This rule is based on the observation that most orally administered drugs have a molecular weight (MW) of five hundred or less, a logP no higher than five, five or fewer hydrogen bond donor sites, and ten or fewer hydrogen bond acceptor sites (N and O atoms). In this study, all the compounds have been found with H donor sites lesser than five and H acceptor sites lesser

than ten. Compounds 10a-N5, 12-N1 and 12f have been predicted with molecular weight more than 500. In addition, the bioavailability of all derivatives was assessed through topological polar surface area analysis. The polar surface area (PSA) was calculated by using topological PSA. This descriptor was shown to correlate well with passive molecular transport through membranes and therefore allows prediction of transport properties of drugs and has been linked to drug bioavailability. Generally, any molecule with PSA value of less  $100 \text{ \AA}^2$  is expected to possess good absorption properties. Passively absorbed molecules with a PSA  $140 \text{ \AA}^2$  are thought to have low oral bioavailability. The PSA value for compounds 12-N1, 12F, N31, N34 are more than  $100 \text{ \AA}^2$  while other studied compounds have lower PSA values (Table 5). Artemisinin has PSA value of  $64.326 \text{ \AA}^2$ . Because of low oil and water solubility of Artemisinin its use in malaria treatment is limited. Derivatives of Artemisinin showed more potency than their parent compound. The parent compound showed CNS toxicity and limited plasma half-life also.

## Conclusion

The present study was carried out to explore predictive QSAR model capable of revealing the structural requirements for potential anti-malarial inhibitors targeting *P. falciparum*. The developed model is significant, robust and has good reliability and predictive ability. The molecular descriptors found in QSAR equation have encoded information about radius of gyration, mominertia Z, SssNH count and SK Average. The compounds N1, N2, N8, N30, N33, and N39 have been predicted with good anti-malarial activities. The docked poses revealed that, all of the derivatives have high binding affinities against parasite plasmepsin-2 and falcipain-2 (hemoglobin digesting enzymes). QSAR model, oral bioavailability, ADME and toxicity risk assessments suggested that compounds N1, N2, N8, N30, N33, and N39 possesses good drug like properties than Artemisinin and DHA. Therefore, the current study advocates the use of combined methodology of QSAR molecular docking and ADME to search potential leads against the *P. falciparum*. The information can be useful for the identification, design and development of diverse, potent anti-malarial with great potential of being drug like compounds.

**Acknowledgement** The author wishes to express gratitude to Prof. B.N. Mishra, Dept. of Biotechnology, IET, Lucknow, for giving inspiring and innovative suggestions.

**Compliance with ethical standards**

**Conflict of interest** The author declares no conflict of interest.

## References

- Avery MA, Muraleedharan KM, Desai PV, Bandyopadhyaya AK, Furtado MM, Tekwani BL (2003) Structure-activity relationships of the antimalarial agent artemisinin. 8. Design, synthesis, and CoMFA studies toward the development of artemisinin-based drugs against leishmaniasis and malaria. *J Med Chem* 46:4244–4258
- Basak SC, Mills D, Garg R, Bhatarai B (2010) A QSAR study of HIV protease inhibitors using theoretical descriptors. *Curr Comput Aided Drug Des* 6:269–282
- Bhatarai B, Garg R (2008) Comparative QSAR as a cheminformatics tool in the design of dihydro-pyranone based HIV-1 protease inhibitors. *Curr Comput Aided Drug Des* 4:283–310
- Cheng F, Li W, Zhou Y et al (2012) AdmetSAR: a comprehensive source and free tool for assessment of chemical ADMET properties. *J Chem Inf Model* 52:3099–3105
- Eckstein-Ludwig U, Webb RJ, van Goethem IDA et al (2003) Artemisinin target the SERCA of *Plasmodium falciparum*. *Lett Nat* 424:957–961
- Ettari R, Bova F, Zappala M, Grasso S (2010) Micale N falcipain-2 inhibitors. *Med Res Rev* 30:136–137
- Fidock DA, Rosenthal PJ, Croft SL, Brun R, Nwaka S (2004) Antimalarial drug discovery: efficacy models for compound screening. *Nat Rev Drug Discov* 6:509–520
- Golenser J, Wakhine JH, Krugliak M, Hunt NH, Grau GE (2006) Current perspectives on the mechanism of action of artemisinins. *Int J Parasitol* 36:1427–1441
- Ibezim E, Duchowicz PR, Ortiz EV, Castro EA (2012) QSAR on aryl-piperazine derivatives with activity on malaria. *Chemomet Intell Lab Syst* 110:81–88
- Kar S, Kar S (2010) Control of malaria. *Nat Rev Drug Discov* 7:511–512
- Liu Y, Cui K, Lu W (2011) Synthesis and antimalarial activity of novel dihydro-artemisinin derivatives. *Mole* 16:4527–4538
- O'Neill PM, Miller A, Bishop LPD et al (2001) Synthesis, antimalarial activity, biomimetic iron (II) chemistry, and in vivo metabolism of novel, potent C-10-phenoxy derivatives of dihydroartemisinin. *J Med Chem* 44:58–68
- Vlife MDS software package, version 3.5 (2008) Supplied by Vlife science technologies Pvt. Ltd, Pune
- Posner GH, Parker MH, Northrop J et al (1999) Orally active, hydrolytically stable, semisynthetic, antimalarial trioxanes in the artemisinin family. *J Med Chem* 42:300–304
- Qidwai T, Yadav DK, Khan F et al (2012) QSAR, docking and ADMET studies of artemisinin derivatives for antimalarial activity targeting plasmepsin II, a hemoglobin-degrading enzyme from *P. falciparum*. *Curr Pharm Des* 37:6133–6154
- Rosenthal PJ, Sijwali PS, Singh A, Shenai BR (2002) Cysteine proteases of malaria parasites: targets for chemotherapy. *Curr Pharm Des* 8:1659–1672
- Schrodinger (2016) Schrodinger Release 2016-4. Schrödinger, LLC, New York
- Trott O, Olson AJ (2010) AutoDock Vina: improving the speed and accuracy of docking with a new scoring function, efficient optimization and multithreading. *J Comput Chem* 31:455–461
- Wang J, Huang L, Li J et al (2010) Artemisinin directly targets malarial mitochondria through its specific mitochondrial activation. *PLoS One* 3:e9582
- World Malaria Report (2013) Global Malaria Programme, WHO, Geneva. [http://www.who.int/malaria/about\\_us/en/](http://www.who.int/malaria/about_us/en/)
- Xiang Y, Zhang Z, Xiao A, Huo J (2009) Recent studies of QSAR on inhibitors of estrogen receptor and human eosinophil phosphodiesterase. *Curr Comput Aided Drug Des* 5:200–214
- Yadav DK, Dhawn S, Chauhan A et al (2014) QSAR and docking based semi-synthesis and in vivo evaluation of artemisinin derivatives for antimalarial activity. *Curr Drug Targets* 8:753–761